Quantum many-body dynamics of 1D Rydberg atom arrays

Oliver Lind
Level 4 Project, MPhys Theoretical Physics
Supervisor: Professor Stuart Adams
Department of Physics, Durham University
Submitted: January 5, 2024

Rydberg atom arrays have allowed isolated quantum many body systems to be investigated like never before. In this study, we carry out numerical simulations of recent exciting equilibrium and non-equilibrium results found on Rydberg arrays. The results are a product of entanglement generating phenomena Rydberg Blockade and allows us to demonstrate quantum phases transition to 1D ordered phases which break discrete symmetries with precise tunability. Moreover, we investigate non-trivial dynamics resulting from quantum quenches to the system and assess new ways of modelling how quantum information propagates through isolated systems.

Contents

I. INTRODUCTION

A. Motivation

Over the past few years, due to advances in optical tweezers technologies, an in flux of experimental studies have come out simulating quantum many body dynamics on Rydberg atom arrays. Experiment tests theory as cold atom simulators simulate dynamics of isolated quantum systems too complex to be programmed on a classical computer.

Recent experiments using Rydberg atom arrays have prompted new studies of quantum critical dynamics around quantum phase transitions as well as realisations of new quantum phases. Moreover, taking thing to the non-equilibrium regime has uncovered unexpected behaviour [1]. In turn, questions surrounding quantum critical phenomena and quantum thermalization have been revisited.

Rydberg atoms possess a singular delocalised electron in a very-highly excited state such that it appears hydrogen-like [2]. Due to their extended coherence times, sensitivity to external fields, and strong dipole-dipole interactions; they have made a great platform for

quantum simulations of many body systems.

In this study, we carry out numerical simulate some of the interesting dynamics found on Rydberg atom arrays and look into quantum information theory for explanations. In particular, attention is brought to how information and entanglement propagate through isolated interacting quantum system as better understanding will aid development of error free Rydberg-atom quantum processors.

B. Transverse Ising Hamiltonian

To set up a model of a programmable cold atom array, N atoms are arranged in an uniform chain of separation a (See Figure 1). Each atom will correspond to a two level system with ground state $|g\rangle$ and excited Rydberg state $|r\rangle$.

The system is driven by lasers such that the two states couple. The strength of the coupling between these two sates is determined by the Rabi frequency Ω and the detuning Δ. For a laser driven on resonance, $\Delta = 0$, the each atom oscillates between ground and Rydberg state at the Rabi frequency. This a result of the quantum optical effect of Rabi oscillations.

In order to generate entanglement and correlations within the system, the atoms need to interact. At distances $\approx 5 - 10\mu$m Rydberg atoms interact strongly with each other through repulsive van der Waals interactions $\propto \frac{1}{a}$. These interaction are factoed into the model and in the next section we discuss how this strong interaction generates entanglement through Rydberg Blockade [3].

Moreover, the system is assumed to be isolated and the boundary conditions open. Combining this all together the dynamics of the N atom chain are encoded into an transverse Ising Hamiltonian [5]:

$$\frac{H}{\hbar} = \frac{\Omega}{2}\sum_i \sigma_i^x - \Delta\sum_i n_i + \sum_{k<i} V_{ik} n_i n_k \quad (1)$$

The first term with operator $\sigma_i^x = |g_i\rangle\langle r_i| + |r_i\rangle\langle g_i|$, couples the ground and Rydberg states. The second term encodes how far detuned the driving laser is from resonance with $n_i = |r_i\rangle\langle r_i|$ the projector on to the Rydberg state. Negative detuning will favor the ground state whereas positive detuning the Rydberg. The last term includes all the Rydberg interactions into the system with $V_{ij} = \frac{C_6}{r^6}$ and $r = a|i-j|$.

Given this Hamiltonian, numerical simulations are run using Trotter-Suzuki decomposition:

$$|\psi(t)\rangle = \prod_{i=1}^{n} e^{-iH(\Omega(t_i),\Delta(t_i))dt_i}|\psi(0)\rangle \quad (2)$$

where $|\psi(0)\rangle$ is the initial state and $dt_i = t_i - t_{i-1}$.

In the model, C_6 = 862690 x 2π MHz μm^6 to resemble the van der Waals interaction of the Rydberg excitation $|r\rangle = |70S_{1/2}\rangle$ of ^{87}Rb which is typically neutral atom of choice for cold atom Rydberg array experiments [4]. Ω = 4 x 2π MHz unless specified otherwise.

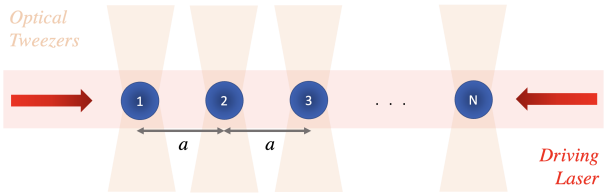

FIG. 1: Set up of 1D Rydberg atom array. Optical tweezers used to trap atoms in place and keep consistent separation a. Uniform Driving Laser of amplitude Ω couples ground state $|g\rangle$ and excited Rydberg state $|r\rangle$

II. TWO ATOM SYSTEM

We look at the two-atom system as a starting avenue for understanding how correlations and entanglement emerge within the system. To simplify things, we set $\Delta = 0$. This leaves Hamiltonian from Eq (4) as:

$$\frac{H_{1,2}}{\hbar} = \frac{\Omega}{2}\sum_{i,j}\sigma_i^x + V_{12}n_1n_2 \tag{3}$$

The dynamics of the system now rely on the scaling between Ω and V_{12}. To analyses, the energies of the optical bare and entangled states: $|00\rangle, |\Psi^-\rangle = \frac{1}{\sqrt{2}}(|00\rangle - |rr\rangle)$, $|\Psi^+\rangle = \frac{1}{\sqrt{2}}(|00\rangle + |rr\rangle)$ and $|rr\rangle$ are plotted against atom separation a in Figure 3.

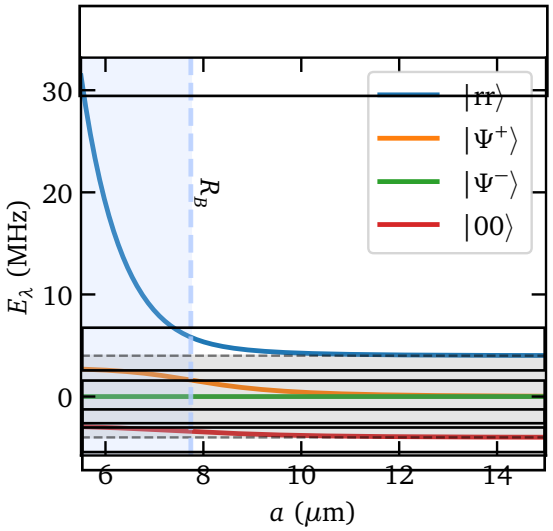

FIG. 2: Energies of two atom bare and entangled states with respect to atomic separation a

First consider the case where $\Omega >> V_{12}$. In this case the Rydberg interaction V_{12} between the two atoms is weak compared to the strength of the driving laser. As a result the Hamiltonian can be considered as separable $H_{1,2} = H_1 + H_2$ and each atom can be treated as a two level systems with oscillations between $|0\rangle$ and $|r\rangle$ at the Rabi frequency, Ω. This corresponds to the region in Figure 3 where states $|00\rangle$ and $|rr\rangle$ have energies E = $-\Omega$ and E = Ω respectively and plus Bell state $|\Psi^+\rangle$ decouples from the resonant driving laser (around $a > 12\mu$m).

The energy of doubly excited Rydberg state, $E_{|rr\rangle}$ grows $\propto \frac{1}{a}$ due to the strong der Waals interactions between excitations. So as a is decreased, $E_{|rr\rangle}$ rapidly increases to energies unreachable by driving laser. As a result at short enough separations, a, our bare states become $|00\rangle$ and $|\Psi^+\rangle$ as the double excitation $|rr\rangle$ becomes blocked of due to high energy requirements. This phenomena is known as Rydberg Blockade and is used to generate entanglement within the system. The characteristic radius at which this effective start to take place, namely the blockade radius, is defined as R_b such that $V_{12} = \frac{C_6}{R_b^6} = \Omega$.

Setting $a = 5.48\mu$m such that $V >> \Omega$ (strong blockade), detuning Δ is now varied. In Figure **??**, bare and entangled states probabilities are plotted against the eigenenergy spectrum for $\Delta = -30$ x 2π MHz to $\Delta = 45$ x 2π MHz to investigate how state couple as a function of detuning.

At large negative detuning $\Delta << 0$, the driving laser is far detuned from the resonant transition to the Rydberg states and hence the system lowest energy eigenstate is firmly $|00\rangle$. As Δ is increased towards zero, the eigenenergies start to come together as the driving laser approaches transition frequency. At transition frequency, Δ = 0, there is a crossing where $|00\rangle$ and $|\Psi^+\rangle$ gradual exchange such that the plus Bell state become the lowest energy eigenstate state of the system for $\Delta > 0$. This transition in populations describes how with positive detuning Rydberg excitations are favoured, but due to blockade energy constraint lowest energy eigenstate can only contain one Rydberg excitation and hence becomes entangled $|\Psi^+\rangle$. As we increases Δ further we encounter another crossing at $\Delta \approx$ 32 x 2π MHz where this time we have exchange between $|\Psi^+\rangle$ and $|rr\rangle$ as $|rr\rangle$ becomes the lowest energy eigenstate. This phenomena

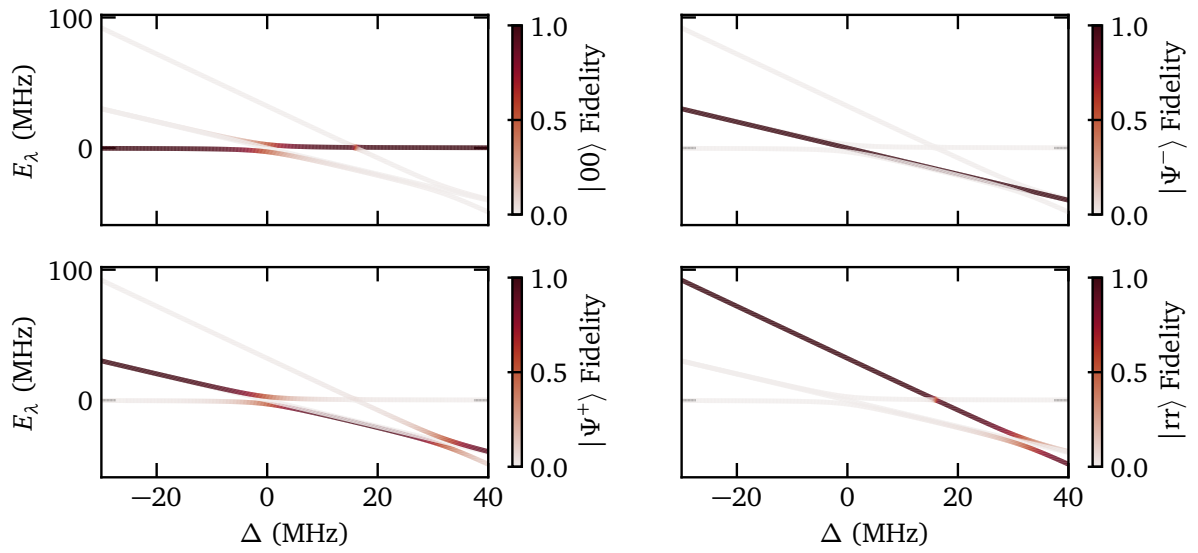

FIG. 3: Eigenenergy spectrum of two atoms separated at a=5.48 μm (strong blockade) as a function of detuning Δ. Colormap indicate fidelities of bare and entangled states across the spectrum

is know as Rydberg anti-blockade and occurs when the energy of our driving laser is high enough such that it overcomes the energy constraint of Rydberg blockade.

The two-atom system has given insight to how the detuning and interaction terms of the Hamiltonian can generate entanglement through Rydberg blockade. Next we look into how dynamics scale as the number of atoms (and thus interactions) is increased and how this can lead to discrete symmetry breaking quantum phases.

III. ADIABATIC QUANTUM PHASE TRANSITIONS

Using the dynamics demonstrated on the two-atom system, Rydberg blockade can be used to engineering specific quantum phases through annealing. This provide insights into how quantum Ising-chain systems behave at quantum critical points and showcases potential of controlled quantum phase transitions in quantum optimisation [6].

The annealing process involves preparing the system in ground state of the initial Hamiltonian H_0 and evolving adiabatically to target Hamiltonian H_1 such that desired ground state is attained. Two cases are investigated with initial Hamiltonian had starting parameters Ω = 4 x 2π MHz and Δ = -30 x 2π MHz such that the ground state of our system corresponds to all atoms in ground state $|0\rangle$. In order to preform phase transitions adiabatically values of detuning Δ will be swept through slow enough such that the system remains in the ground states of the evolved Hamiltonian. Varying Δ to quickly would elicit non-adiabatic transitions to higher energy eigenstates and introduce topological defects into our system.

A. Rydberg Crystals

The Rydberg Blockade effect has allowed for a multitude of spatial ordered 1D and 2D quantum phases ('Rydberg Crystals') to be realised on optical lattice simulators which break discrete symmetries on up to 256-atoms [7]. Using Numerical Simulations, we demonstrate how these crystalline states are realised on 1d arrays.

Two separate cases of 7 atoms with atomic

separations, a = 5.48 μm, 3.16 μm respectively are considered. Both systems are evolved by the same linear detuning sweep through Δ = 0 MHz to high detuning Δ = 30 x 2π MHz (See Figure 4). At the end of the sweep, for a = 5.48 μm, $V_{i,i+1} > \Delta >> \Omega >> V_{i,i+2}$ such that there is nearest neighbour blockade. Instead for a = 3.16 μm, $V_{i,i+2} > \Delta >> \Omega >> V_{i,i+3}$ there is next-to-nearest neighbour blockade. In Figure 5, results of both simulations are shown.

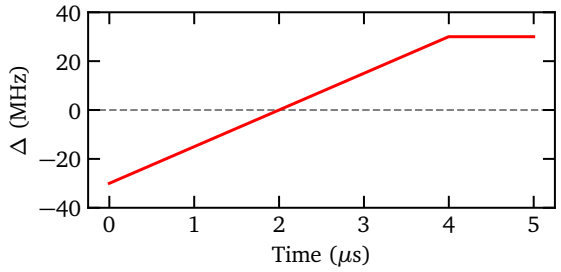

FIG. 4: Adiabatic detuning sweep

At positive detuning, $\Delta > 0$, spatially ordered phase emerge as detuning favours a Rydberg excitations whilst Blockade effect prohibits excitations of atoms within the blockade radius R_b. For case of nearest-neighbour blockade, a = 5.48 μm, neighbouring atoms cannot be simultaneously excited. This leads to the formation of the anti-ferromagnetic (AF) or Z_2 ordered state $|r0r0...\rangle$. On even N arrays the Z_2 state is two-fold degenerate due to symmetry of the system. However, for odd N array systems Z_2 state with edge excitations $|r0r..0r\rangle$ is favoured over other $|r0r..0r\rangle$ as maximises Rydberg excitations subject to the blockade constraint. As a result, when referring to the AF or Z_2 state on odd N arrays we will mean the state with edge excitations unless specified otherwise. Similarly, for a = 3.16 μm, due to next-to-nearest neighbour blockade the Z_3 ordered state forms as three neighbouring atoms are restricted to one excitation. In Figure 5, we see these ordered states emerge with high fidelity.

IV. NON EQUILIBRIUM DYNAMICS

Following our discussion of adiabatic QPTs, we now do the opposite and study what happens the Hamiltonian of the system is perturbed fast enough such that the system is forced into a non-equilibrium regime. This sudden change in the Hamiltonian as know as a quantum quench. We show that, despite the aggressive nature of a quench, ordered behaviour emerges in the non-equilibrium system.

To perform quenches, rapid changes to laser detuning Δ modify the Hamiltonian. We note that this is not the only way to preform a quench with other options such as at rapidly changing separation, a. However, it is the most experimentally feasible and has been done on 1D arrays up to 51 atoms [1].

A. Global Quench

To start, the 3 atom Z_2 state $|r0r\rangle$ is quench from high positive detuning (equilibrium Hamiltonian configuration). This is done by evolving to the Z_2 state by detuning sequence to Δ = 30 x 2π MHz and quenching to Δ = 0 MHz. As demonstrated in Figure 6a, after the quench order oscillations between initial state $|r0r\rangle$ and $|0r0\rangle$ emerge. The order of these oscillations are not exactly known. Given that Ω is a conserved quantity of our system we would expect the oscillation at similar frequency. However, it turn out the dynamics are more complex and this is not the case with multiple frequencies contributing to the Z_2 oscillations revival.

To get a better understanding, we look at how the eigenenergies of the system evolve. In Figure 6b, for the detuning sweep (between t = 0 μs and t = 4 μs) the system if firmly in the ground eigenstate of the system. But when the system is quenched (t = 4μs), it's state

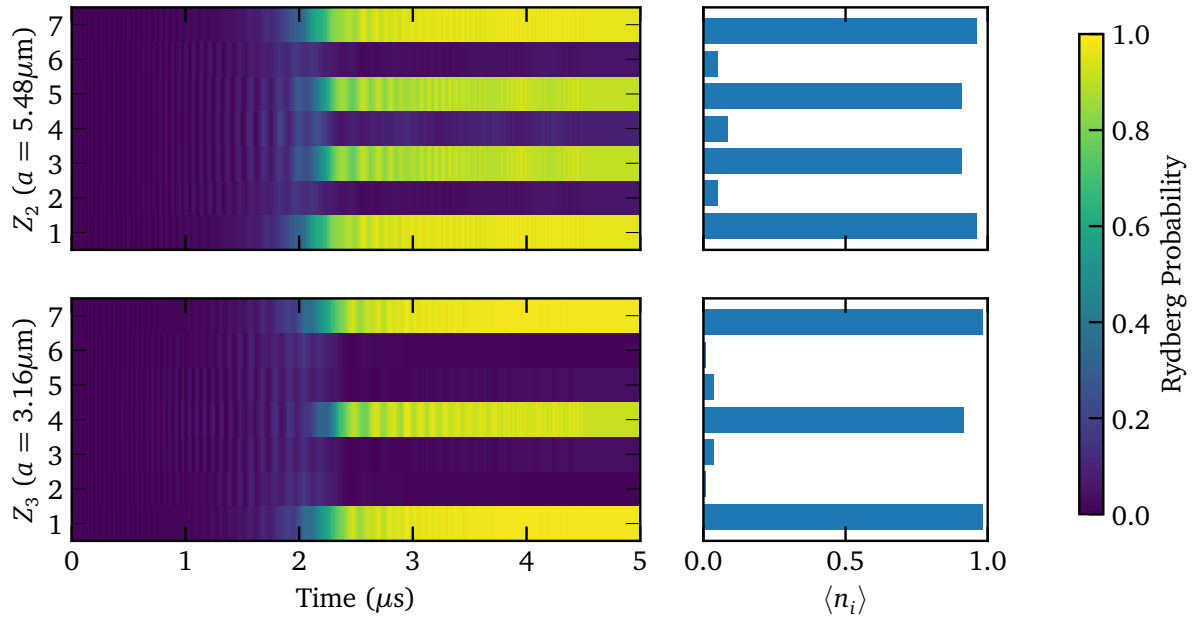

FIG. 5: Rydberg excitation probability colormap. For each time step dt=0.01μs and each individual atomic site i, Rydberg excitation probabilities are calculated through expectation value $\langle n_i \rangle$ where $n_i = |r_i\rangle \langle r_i|$ is the projector onto the Rydberg state. Bar charts show final Rydberg excitation probabilities after the sweep.

spreads over four eigenstates and becomes a superposition of them. This mechanism can be understood through Heisenberg's uncertainty principle. By quenching, energy is put into the system as the negative second term of the Hamiltonian Eq (1) jumps up to zero. This impulse of energy sends the quantum state to a higher energy eigenstate before the Hamiltonian can respond (non-adiabatic transition). But, due to the short time interval this happens at dt=0.01μs (time step of simulation), this results in a spread ΔE of possible energies the system is in by Heisenberg's uncertainty principle. As a result, the state of the system projected across eigenstates. One would then expect the result behavior to be rather disordered as multiple eigenenergies induce multiple different oscillation frequencies. However, it turns out there are 'special' initial states which retain information about there initial conditions for long times after quenching. The order Z_2 is found to be one of them [8].

Scaling up to 7 atoms, similar quantum scar behaviour holds (See Figure [**?**]). Here, the initial Hamiltonian is set at high positive detuning, Δ = 30 x 2π MHz, with initial ground state $|r0r0r0r\rangle$ and quenched such that Δ=0 instantaneously.

This quantum scar effect is of great interest in both a theoretical and application sense. Theoretically, the quantum scar effect is interesting as it revisits the age old question as to how and when isolated quantum systems thermalize? Quantum thermalization is the processes by which isolated quantum systems out of equilibrium thermally equilbrate by acting as their own thermal reservoir such that local observable tend to values predicted by equilibrium ensembles. This mechanism is described by eigenstate thermalization hypothesis (ETH). Quantum scars are examples of behavior that breaks ETH as the initial state of the system is retain for many revivals As a result quantum scar could provide a useful way of retaining memory.

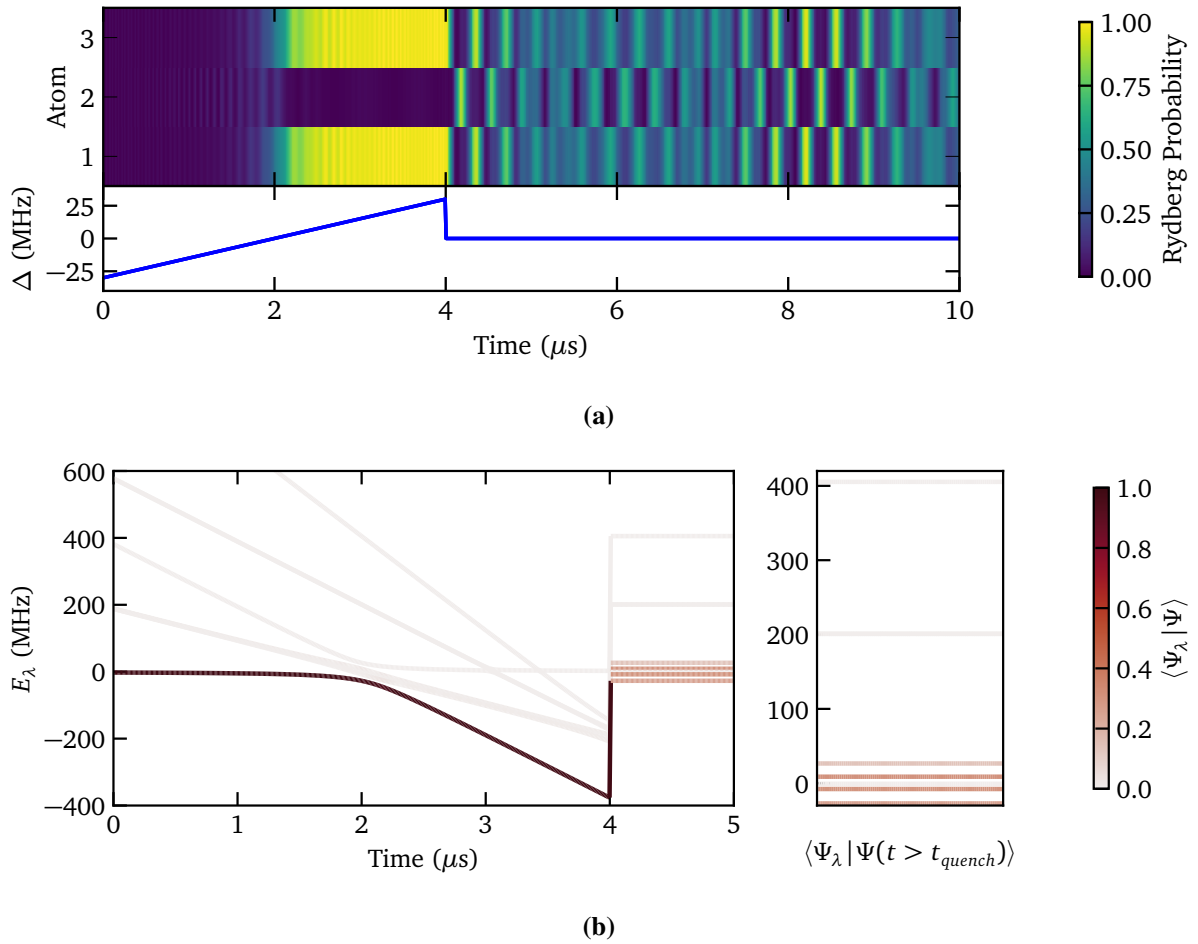

FIG. 6: Figures showing dynamics of global quench on 3 atom system by driving $\Delta_{initial}$ = 30 x 2π MHz to Δ_{quench} = 0 MHz. **(a)** Rydberg excitation probability colormap, dt=0.01μs. **(b)** Eigenenergies of Hamiltonian across sweep and quench with colormap to show distribution of quantum state $|\psi(t)\rangle$ across the spectrum

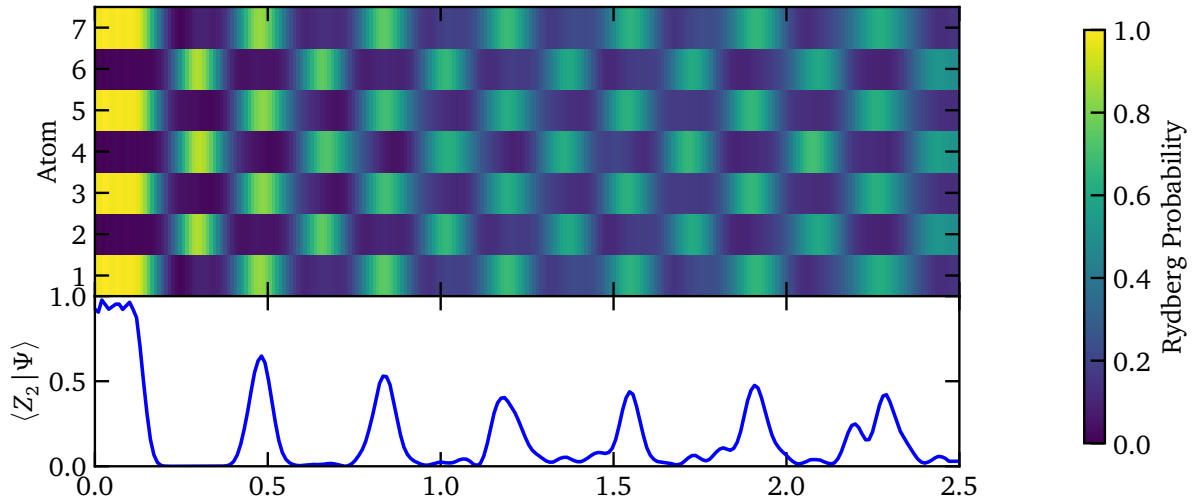

FIG. 7: Rydberg excitation probability colormap, dt=0.01μs for Global quench on 7 atom system ($\Delta_{initial}$ = 30 x 2π MHz, Δ_{quench} = 0 MHz)

B. Local Quench

So far all atoms in the system have been addressing globally. Now, we investigate what happens when we only quench a subset of atoms in the chain and unveil insights into how information and entanglement propagates through strongly interacting systems. In order to do so the Hamiltonian is modified to allow for single site addressing:

$$\frac{H}{\hbar} = \frac{\Omega}{2}\sum_i \sigma_i^x - \sum_i \Delta_i n_i + \sum_{k<i} V_{ik} n_i n_k \quad (4)$$

Moreover, in order to quantify how information spread across the system we consider the quantum mutual information between two sites i and j given by [9]:

$$\begin{aligned} I(i,j) &= S_{vN}(\rho_i) + S_{vN}(\rho_j) - S_{vN}(\rho_{ij}) \\ &= S_{vN}(\rho_{ij}||\rho_i \otimes \rho_j) \end{aligned} \quad (5)$$

where $\rho_i = tr_{k\neq j}(|\Psi\rangle\langle\Psi|)$, $\rho_j = tr_{k\neq i}(|\Psi\rangle\langle\Psi|)$ and $\rho_{ij} = tr_{k\neq i,j}(|\Psi\rangle\langle\Psi|)$ are the reduced density matrices at for subspaces H_i, H_j and H_{ij} respectively; $S_{vN}(\rho)$ is the von Nuemann entropy and $S_{vN}(\rho_{ij}||\rho_i \otimes \rho_j)$ is the quantum relative entropy.

The quantum relative entropy tell us how distinguishable two density matrices are. Therefore by Eq (5), quantum mutual information tells us how distinguishable the (reduced) density matrices ρ_{ij} and $\rho_i \otimes \rho_j$ are which correspond to how correlated subspaces H_i and H_j.

For example, in a two atom system if $I(1,2)$=0 then ρ_{ij}=$\rho_i \otimes \rho_j$ which says that the system is separable and hence there is no entanglement between the two atoms. But if $I(1,2) > 0$ then $\rho_{ij} \neq \rho_i \otimes \rho_j$ (they are distinguishable) and the system is not separable and hence the two atoms are entangled. For larger N, $I(i,j) > 0$ does not necessarily imply entanglement but correlation.

1. *Quenching 1st Atom*

We begin by considering what happens when we quench only the first atom in the chain. The system is set up as before with initial Hamiltonian $H(\Omega$= 4 x 2π, Δ= 30 x $2\pi)$ in initial Z_2 state $|r0r0r0r\rangle$ (ground). Instead of quenching all the atoms, at $t = t_{quench}$: Δ_1= 0 and $\Delta_i \neq 1$= 30 x 2π instanaeously.

Plotting the resulting Rydberg state probabilities we notice the quench at atom 1 results in change to the entire system (See Figure [].

Figure 8 shows results of such a quench which despite beging local results in change across the whole system. In particular, there is a delay in the time it take for atom seven to change after quench at atom one and it appears there is some finite speed at which information propagates throughout the system.

To explore this further, quantum mutual information between atom 1 and the rest right after the quench is considered. Result are shown in Figure 9. There is a clear speed at which correlations are propagating through the system as correlations take a finite time to reach atom seven. Moreover, the strength of the correlations decay further down the chain.

These result matches behaviour expected by the Lieb-Robinson Bound [10]. The Lieb-Robinson Bound is an upper limit how fast information can propagate in a quantum system obeying the Schrodinger equation with local interactions. With this is mind we can look into describing the post quench dynamics through that of a quasi-particle travelling within the L-B bound [11]. Developing our understanding of this will pave the way to realising Rydberg-atom array quantum information processors as understanding how information and entanglement propagates through these systems is crucial to finding ways to reduce the effects of errors.

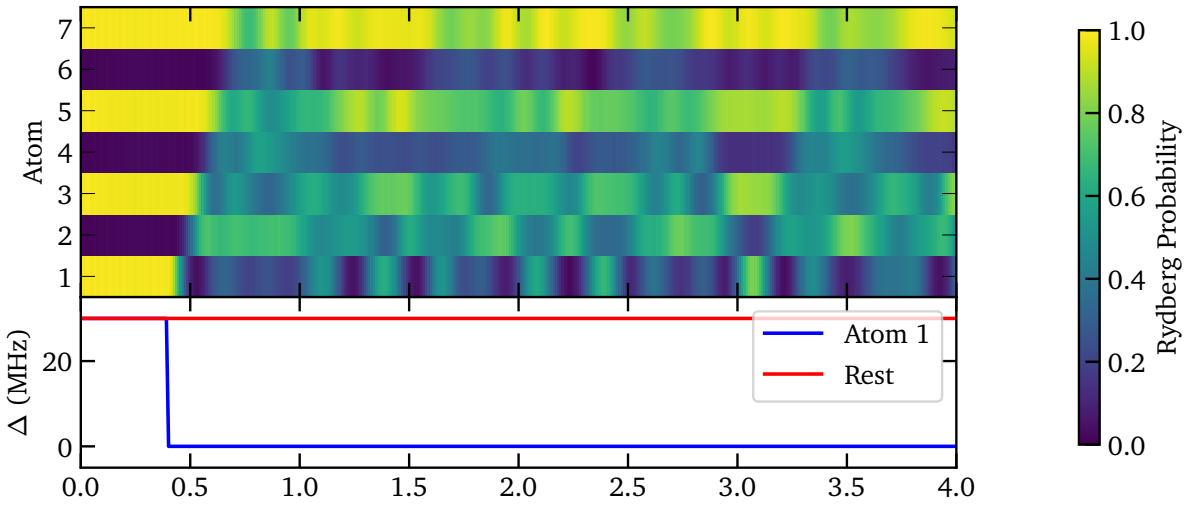

FIG. 8: Rydberg excitation probability colormap, dt=0.01μs for local quench on atom 1 of 7 atom system ($\Delta_{initial}$ = 30 x 2π MHz, $\Delta_{1,quench}$ = 0 MHz, $\Delta_{2-7,quench}$ = 30 x 2π MHz

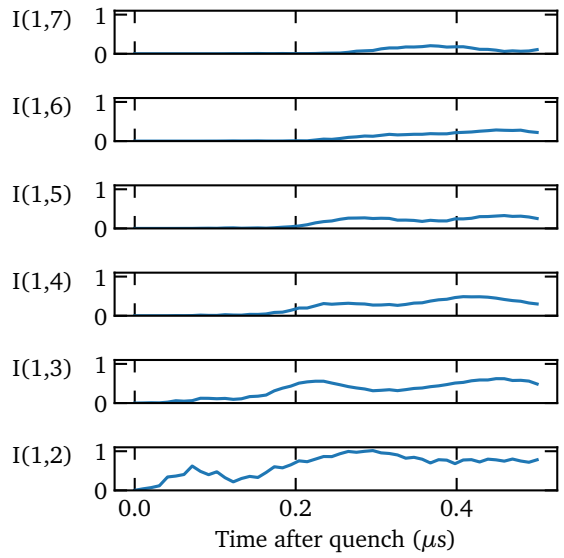

FIG. 9: Quantum Mutual Information between atom 1 and rest of 7 atom system after local quench on atom 1

V. CONCLUSIONS

Overall, we demonstrate how strongly interacting Rydberg atoms can generate entanglement between each other and how this can lead to order quantum phases on 1D arrays allowing for further study of quantum critical phenomena. Moreover, we look at the interesting non-trivial dynamics of ordered phases brought suddenly out of equilibrium through a quantum quench. This introduce the weak-ergodicity breaking phenomena of quantum many body scars associated with the periodic revival of the initial state. Additionally, through locally quenching atoms in the array, we study how information and entanglement propagate across the system - necessary to developing error free Rydberg-atom quantum information processors.

[1] Bernien, Hannes, Sylvain Schwartz, Alexander Keesling, Harry Levine, Ahmed Omran, Hannes Pichler, Soonwon Choi, et al. "Probing Many-Body Dynamics on a 51-Atom Quantum Simulator." Nature News, November 30, 2017. https://www.nature.com/articles/nature24622.

[2] Adams, Charles, and Nikola Šibalić. Rydberg Physics. IOP Publishing Limited, 2018.

[3] Urban, E., T. A. Johnson, T. Henage, L. Isenhower, D. D. Yavuz, T. G. Walker, and M. Saffman. "Observa-

tion of Rydberg Blockade between Two Atoms." Nature News, January 11, 2009. https://www.nature.com/articles/nphys1178.

[4] "Bloqade." Home · Bloqade.jl. Accessed January 5, 2024. https://queracomputing.github.io/Bloqade.jl/stable/.

[5] Labuhn, Henning, Daniel Barredo, Sylvain Ravets, Sylvain de Léséleuc, Tommaso Macrì, Thierry Lahaye, and Antoine Browaeys. "Tunable Two-Dimensional Arrays of Single Rydberg Atoms for Realizing Quantum Ising Models." Nature News, June 1, 2016. https://www.nature.com/articles/nature18274.

[6] Kim, Minhyuk, Jaewook Ahn, Yunheung Song, Jongchul Moon, and Heejeong Jeong. "Quantum Computing with Rydberg Atom Graphs - Journal of the Korean Physical Society." SpringerLink, March 13, 2023. https://link.springer.com/article/10.1007/s40042-023-00774-1.

[7] Ebadi, Sepehr, Tout T. Wang, Harry Levine, Alexander Keesling, Giulia Semeghini, Ahmed Omran, Dolev Bluvstein, et al. "Quantum Phases of Matter on a 256-Atom Programmable Quantum Simulator." arXiv.org, December 22, 2020. https://arxiv.org/abs/2012.12281.

[8] Serbyn, Maksym, Dmitry A. Abanin, and Zlatko Papić. "Quantum Many-Body Scars and Weak Breaking of Ergodicity." Nature News, May 27, 2021. https://www.nature.com/articles/s41567-021-01230-2.

[9] Kumar, Asutosh. "Multiparty Quantum Mutual Information: An Alternative Definition." arXiv.org, July 28, 2017. https://arxiv.org/abs/1504.07176.

[10] Lieb, Elliott H., and Derek W. Robinson. "The Finite Group Velocity of Quantum Spin Systems." Communications in Mathematical Physics 28, no. 3 (1972): 251–57. https://doi.org/10.1007/bf01645779.

[11] Schachenmayer, J., B. P. Lanyon, C. F. Roos, and A. J. Daley. "Entanglement Growth in Quench Dynamics with Variable Range Interactions." Physical Review X, September 13,2013. https://journals.aps.org/prx/abstract/10.1103/PhysRevX.3.031